Available online at www.sciencedirect.com
SCIENCE DIRECT
Thermochimica Acta 414 (2004) 233–241
thermochimica acta
www.elsevier.com/locate/tca

Microcalorimetry, energetics and binding studies of DNA–dimethyltin dichloride complexes

A.A. Moosavi-Movahedi [a,d,*], A.R. Golchin [b], K. Nazari [c], J. Chamani [a], A.A. Saboury [a], S.Z. Bathaie [e], S. Tangestani-Nejad [f]

[a] *Institute of Biochemistry and Biophysics, University of Tehran, P.O. Box 13145-1384, Tehran, Iran*
[b] *Department of Chemistry, Science and Research Campus, Islamic Azad University, Tehran, Iran*
[c] *Chemistry and Petrochemical Division, Research Institute of Petroleum Industry, Tehran, Iran*
[d] *Center of Excellence for Interdisciplinary Sciences, IAU, Tehran, Iran*
[e] *Department of Clinical Biochemistry, Tarbiat Modares University, Tehran, Iran*
[f] *Department of Chemistry, Faculty of Science, University of Isfahan, Isfahan, Iran*

Received 23 July 2003; received in revised form 7 January 2004; accepted 7 January 2004

Abstract

The interaction of dimethyltin dichloride (Me_2SnCl_2) with calf thymus DNA was studied at 27 °C, pH 7.6 using various techniques including isothermal titration calorimetry (ITC) and UV-Vis, fluorescence and IR spectrophotometries. The binding isotherm and enthalpy curve for Me_2SnCl_2–DNA interaction was a biphasic transition process. This was determined by the analysis of the binding data with the Hill equation. The first phase of the enthalpy curve (exothermic process) was consistent with the first set of binding site, the second phase (endothermic process, less exothermicity) was consistent with second set of binding site from the cited interactions. Our results showed that the first set of binding sites is occupied by one mole of ligand bound per near 1 base pair of DNA. The DNA–ethidium bromide (EB) complex, in the presence of Me_2SnCl_2, caused the quenching of the fluorescence emission. The Scatchard plots illustrated a non-intercalating manner for such quenching. The DNA–EB complex results indicated that the binding of Me_2SnCl_2 is with the phosphate groups of DNA at low ligand concentrations (<9 mM). This was confirmed with the IR spectrophotometric spectra. However, the binding at higher ligand concentrations (>9 mM) was with the base groups of DNA. Therefore, these results suggest that the Me_2SnCl_2 binding to DNA at low concentrations occurs through an outside interaction by an exothermic process. However, the partial unfolding of the DNA caused at higher concentrations of Me_2SnCl_2 is through an endothermic process involving interactions with the base groups.

Keywords: DNA; Dimethyltin dichloride; Enthalpy change; Binding sites analysis; Microcalorimetry; Noncompetitive interaction

1. Introduction

The use of modern techniques for structural studies has increased our understanding of the cell function at molecular levels. One of the most important aims of modern biology is to understand the cell function in terms of the structure and interactions of its constituents, namely the DNA, RNA, proteins and lipids.

All forms of DNA have negative charge on their surface, so that they interact readily with positive charged molecules such as proteins (histones) [1], peptides [2], polyamines [3,4], metals [5], cationic lipids and liposomes [6–10], as well as monovalent cationic surfactants [11–22]. The significance of metal binding to nucleic acids involved in DNA replication, transcription, messenger RNA translation is well established [23–25]. The action of metal ions in the stabilization of the tertiary structure of tRNA shifts the thermally induced helix-coil transition of DNA to higher temperatures T_m [26,27]. Metal ions, however can also have a destabilizing effect on DNA double–helical structure if they interact with bases rather than with the phosphate groups. In the series Mg, Co, Ni, Mn, Zn, Cd, Cu, the affinity for base complexation relative to phosphate binding increases from left to right.

In principle, three different groups of metal containing antitumor agents can be distinguished. Inorganic complexes composed of a central metal atom surrounded by inorganic

* Corresponding author. Tel.: +98-21-6403957; fax: +98-21-6404680.
E-mail address: moosavi@ut.ac.ir (A.A. Moosavi-Movahedi).

0040-6031/$ – see front matter © 2004 Elsevier B.V. All rights reserved.
doi:10.1016/j.tca.2004.01.007

ligands (the most famous example of inorganic cytostatics is cis-diaminedichloroplatinum(II) (cisplatin)). Organometallic complexes containing one or more metal atoms as well as organic, the ligands being linked to the metal by direct carbon–metal bonds (many of the non-platinum group as the metal antitumor agents known are typical organometallic compounds). Complexes also including metal atoms and organic ligands without carbon–metal bonds are not defined as organometallic [28]. In general, the organotin(IV) compounds of the type R_2SnX_2 tested so far against the p388 lymphocytic leukemia in mice, showed only marginal activity [29]. organotin(IV) compounds are known to exhibit important cytotoxic effects and are actively investigated as possible antitumor compounds [30–32]. It was previously suggested that organotin(IV) compounds exert their effects through binding to thiol groups of protein [33]. In contrast to this view, but in analogy with the behavior of several antitumor metal complexes, others have proposed that DNA is the probable target for the cytotoxic activity of organotin compounds [34]. Organotin compounds are widespread in the environment [35], interact with living organism [36], and widely used [37].

The interaction of Sn(IV)Me_2 moieties with native DNA has recently been investigated, to provide a molecular basis for the understanding of the biological effects of organotin(IV) derivatives [38]. It is reported the bonding and structures of organotin(IV)–deoxyribonucleic acid (DNA) condensates by ^{119}Sn Mössbauer spectroscopy [39]. DNA condensation is mainly due to electrostatic interactions between Sn(IV)R_n moieties(n = 1–3) and phosphodiester groups of DNA [39]. SnR_2(DNA phosphodiester)$_2$ (R = Me, Et) and $SnEt_3$(DNA phosphodiester) stoichiometries have been determined in lyophilized condensates by variable-temperature 119 Mössbauer spectroscopy [40]. The existence of octahedral $SnR_2(H_2O)[O_2P(OR')_2]$, and trigonal bipyramidal $SnR_3(H_2O)[O_2P(OR')_2]$ tin environments, have been established by point-charge modeling of the 119 Mössbauer nuclear quadrupole splittings [39,40]. These findings indicate the existence of solid-state complex of Sn(IV)R_2 and Sn(IV)R_3 moieties with mononucleotides and phenylphosphates [41]. Moreover, 119 Mössbauer studies in aqueous solutions at natural pH (frozen to 77.3 K) indicate that $SnMe_2(OH)_2$ and $SnMe_3(OH)$ are coordinated by phosphate and D-ribose-5-phosphate [42]. Potentiometric studies in aqueous solutions (pH = 6.5) gave evidence for the formation of 1:1 complexes between $SnMe_3(H_2O)_2$ and adenosine or inosine 5′-monophosphates through phosphate oxygens [43]. Also an extensive study to elucidate the Sn(IV)Me_3, Sn(IV)Me_2 and Sn(IV)Me moieties interacting with DNA in aqueous solution using small-angle X-ray scattering (SAXS), circular dichroism and variable—temperature UV spectroscopy, in order to investigate the influence of methyltin(IV) chlorides on the secondary structure of DNA in its native form is reported [40]. In the present study, we have investigated the binding and thermodynamic aspects of interactions of dimethyltin dichloride (Me_2SnCl_2) with DNA to obtain DNA structural information.

2. Materials and methods

2.1. Materials

Dimethyltin dichloride (Me_2SnCl_2) (>97%) and high molecular weight calf thymus DNA (cat no. 24013) were obtained from Merck. All other materials used were of analytical grade. All the experiments were carried out in 0.01 M phosphate buffer, pH 7.6 at 27 °C. The DNA concentrations were determined using an extinction coefficient of 13200 M^{-1} cm^{-1} at 260 nm and expressed in terms of base pair molarity (mM bp) [44]. All solutions were prepared with deionized water (Barstead Nanopure ER = 18.3 MΩ).

2.2. Methods

2.2.1. Isothermal titration calorimetry (ITC), heat measurement

Enthalpy measurement was made at 27 °C using microcalorimeter (2277 thermal activity monitor, Thermometric, Sweden). The microcalorimeter was interfaced with an IBM PS/2 Model 40486 computer, using thermometric Digitam 3 software program. Each channel is a twin heat-conduction calorimeter where the heat-flow sensor is a semiconducting thermopile (multi junction thermocouple plates) positioned between the vessel holders and the surrounding heat sink. The insertion vessel was made from stainless steel. Me_2SnCl_2 solutions were injected by using of a Hamilton syringe into the calorimetric stirred titration vessel, which thin (0.15 mm inner diameter) stainless steel hypodermic needles, permanently fixed to the syringe, reached directly in to the calorimeter vessel. The injection of Me_2SnCl_2 in to the perfusion vessel was repeated 20 times. The speed of stirring was 20 cycle/min and titration pump was motor-driven. The calorimetric signal was measured with a digital voltmeter, part of a computerized recording system. The enthalpy change of interaction between Me_2SnCl_2 and DNA was measured at <1.2 and >1.2 mM of ligand by transferring of 40 μl (in each injection) of 3.7 and 55 mM of Me_2SnCl_2 to the 1.8 ml of DNA solution (0.0242 mM base molarity, mM bp), respectively. The enthalpy change of dilution of Me_2SnCl_2 was corrected by measuring the enthalpy change of each injection into buffer solution. The heat released by DNA dilution was negligible. The microcalorimeter was calibrated electrically during the course of the study.

2.2.2. Fluorescence measurement

The fluorescence measurement was carried out by a Hitachi model RF-5000 spectrofluorimeter. The instrument was operated in the energy mode. Both slit widths employed were 10 nm for the excitation and emission beam. The

spectra were recorded at 10 nm/min scanning speed without filter. The emission spectrum of ethidium bromide (EB) were studied at $\lambda_{excitation} = 480$ nm and $\lambda_{emission} = 600$ nm. The fluorimetric study of the interaction of EB with DNA in the absence and presence of Me_2SnCl_2 was investigated to the method reported by Strothkamp and Strothkamp [45].

2.2.3. Binding measurement

Titration difference spectrophotometry was carried out using a Camspec Model M-350, double-beam spectrophotometer. The interaction of DNA with various concentrations of Me_2SnCl_2 (0.05–16 mM) was studied using spectrophotometric method. The wavelengths of 435 and 260 nm were used at low concentrations (<9 mM) and high concentrations (>9 mM) of Me_2SnCl_2 upon interaction with DNA, respectively.

The binding constant of Me_2SnCl_2 to DNA at low concentrations was obtained from spectrophotometric titration using the Benesi–Hildebrand expression [46]:

$$\frac{1}{\Delta A} = \left(\frac{K_d}{\Delta A_\infty}\right) \times \frac{1}{[S]} + \left(\frac{1}{\Delta A_\infty}\right) \quad (1)$$

$$\Delta A_\infty = \varepsilon b[\text{DNA}] \quad (2)$$

where K_d is the dissociation constant of the DNA–ligand complex, ΔA is the difference observed absorbance change at wavelength of 435 nm in the presence and the absence of Me_2SnCl_2, ΔA_∞ is the maximum absorbance change and $[S]$ represents the ligand concentration. ε is the molar absorptivity (extinction coefficient) of the complex and b is the light path-length of the cell (1 cm). Eq. (1) indicates linear changes of $1/\Delta A$ versus $1/[S]$ with Y-intercept of $1/\Delta A_\infty$ and slope of $K_d/\Delta A_\infty$. Thus, K_d could be determined from the slope of the plot via linear regression.

Binding data can be obtained by estimating the concentration of bound ligand using Eq. (3):

$$[Me_2SnCl_2]_{bound} = \frac{\Delta A}{\varepsilon_{435}} \quad (3)$$

where ε_{435} is equal to $2.174 \times 10^3\ cm^{-1}\ M^{-1}$ and could be obtained from Fig. 1b and Eq. (2).

Substitution of $[Me_2SnCl_2]_{bound}$ into Eq. (4) leads to determination of free ligand concentration:

$$[Me_2SnCl_2]_{total} = [Me_2SnCl_2]_{free} + [Me_2SnCl_2]_{bound} \quad (4)$$

Finally, ν is obtained from Eq. (5):

$$\nu = \frac{[Me_2SnCl_2]_{bound}}{[\text{DNA}]} \quad (5)$$

Also binding data could be analyzed based on the Scatchard plot according to Eq. (6):

$$\frac{\nu}{[Me_2SnCl_2]_{free}} = K(n - \nu) \quad (6)$$

where ν, K and n are the number of mole of ligand per molar base pair of DNA, equilibrium binding constant and the number of binding sites, respectively. Binding parameters (ν and K) for cited interactions at higher concentrations of Me_2SnCl_2 (>9 mM) were obtained in a similar manner at wavelength of 260 nm using Eqs. (3)–(6). The molar extinction coefficient (ε_{260}) of Me_2SnCl_2–DNA complexes was equal to $13220\ M^{-1}\ cm^{-1}$ and can be obtained from Eq. (2) and A_∞ is obtained from saturation state in the denatured position of the sigmoidal curve (see Fig. 1c). The binding parameters (g and n_H) were obtained by fitting of the experimental data into the Hill equation using the Sigma-Plot software. These values are tabulated in the Table 1. g is the maximum number of binding site and n_H is Hill coefficient.

2.2.4. IR spectrophotometry

The IR spectra were recorded on a Bomem MB-100 Fourier transform IR instrument. IR spectra (resolution = $4\ cm^{-1}$, 20 scans per spectrum) were prepared for solutions of DNA–Me_2SnCl_2 complexes using a cell with CaF_2 windows, at low concentrations of Me_2SnCl_2 (2.2 mM). The concentration of DNA was 24.2 mM bp. The IR spectra of Me_2SnCl_2–DNA at high concentration of Me_2SnCl_2 cannot be recorded because of the solid gel formation. It is also reported that, the addition the organotin(IV) chloride from 0.1 M concentrated ethanol solution, to aqueous native DNA at neutral pH, induces DNA condensation with the formation gel phases, interpreted as the neutralization of the negative charge of phosphodiester groups by cationic organotins [39,40]. Hence, it can be concluded that in the solutions at low concentrations of DNA monomer and organotin chloride used here, organotin moieties could interact with both phosphodiester groups and H_2O.

Table 1
Binding sites parameters for DNA–Me_2SnCl_2 complexes at 27 °C

Sets	g_1	g_2	g_3	g_4	n_{H1}	n_{H2}	n_{H3}	n_{H4}	K_1	K_2	K_3	K_4
Set 1												
Site 1	0.5	–			1.1	–			6378	–		
Site 2	–	1			–	3.49			–	3235		
Set 2												
Site 1			1.3	–			1.5	–			3226	–
Site 2			–	1.6			–	3.99			–	29.3

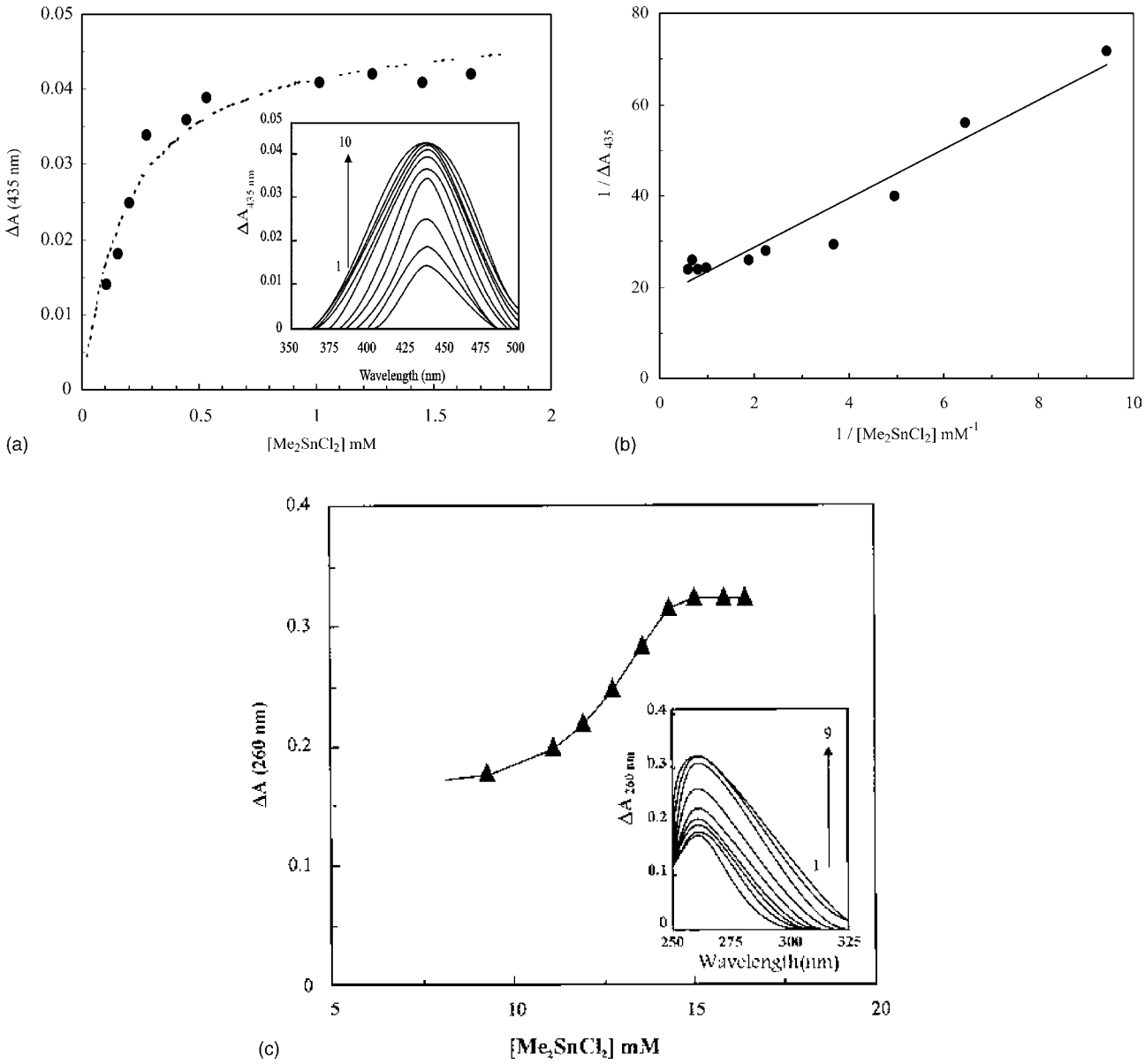

Fig. 1. (a) Titration of DNA (0.0242 mM bp) with Me_2SnCl_2, $\varepsilon_{435} = 2.174 \times 10^3\ M^{-1}\ cm^{-1}$ was used for the calculation of Me_2SnCl_2–DNA complex at low concentrations of ligand at pH 7.6. The absorbance (ΔA) of Me_2SnCl_2–DNA complex from concentration of >1.5 up to 9 mM of Me_2SnCl_2 is near constant (data not plotted). (●) Experimental data, dashed curve is obtained by fitting using Eurika program. (a: inset) The visible spectra of the interaction of DNA with Me_2SnCl_2 at 435 nm (<9 mM): (1) 0.106 mM Me_2SnCl_2; (2) 0.155 mM Me_2SnCl_2; (3) 0.202 mM Me_2SnCl_2; (4) 0.272 mM Me_2SnCl_2; (5) 0.444 mM Me_2SnCl_2; (6) 0.53 mM Me_2SnCl_2; (7) 1.011 mM Me_2SnCl_2; (8) 1.235 mM Me_2SnCl_2; (9) 1.4 mM Me_2SnCl_2; (10) 1.62 mM Me_2SnCl_2. (b) Reciprocal plot based on Eq. (1) and estimation of K_d for Me_2SnCl_2–DNA complex. Slop $= K_d/\Delta A_\infty = 5.3431$, Y-intercept $= 1/\Delta A_\infty = 18.994$. (c) The titration profile of DNA at 260 nm in the presence of high concentrations of Me_2SnCl_2 (up to 16 mM) at pH 7.6. The molar extinction coefficient (ε_{260}) of Me_2SnCl_2–DNA complexes is equal to $13220\ M^{-1}\ cm^{-1}$. (c: inset) The UV spectra of the DNA interactions with Me_2SnCl_2 at 260 nm: (1) 9.3 mM Me_2SnCl_2; (2) 11.2 mM Me_2SnCl_2; (3) 11.98 mM Me_2SnCl_2; (4) 12.9 mM Me_2SnCl_2; (5) 13.6 mM Me_2SnCl_2; (6) 14.2 mM Me_2SnCl_2; (7) 14.8 mM Me_2SnCl_2; (8) 15.5 mM Me_2SnCl_2; (9) 16.2 mM Me_2SnCl_2.

3. Results and discussion

3.1. Binding data

The difference absorption spectra of DNA–Me_2SnCl_2 complex at 435 nm is shown at the presence of low concentrations of dimethyltin dichloride (Me_2SnCl_2) (<9 mM) in Fig. 1a (inset). Fig. 1a depicted the titration difference absorbance curve at 435 nm for DNA upon interaction with Me_2SnCl_2 at low concentrations (<9 mM). Based on Eq. (1) and from the double reciprocal plot, the dissociation equilibrium constant (K_d) can be obtained. The extinction coefficient for such interaction can be obtained from Eq. (2) (see Fig. 1b). The values of K_d and ε were equal to 2.81×10^{-4} M and $2.174 \times 10^3\ cm^{-1}\ M^{-1}$, respectively. Fig. 1c is shown the titration difference absorbance profile

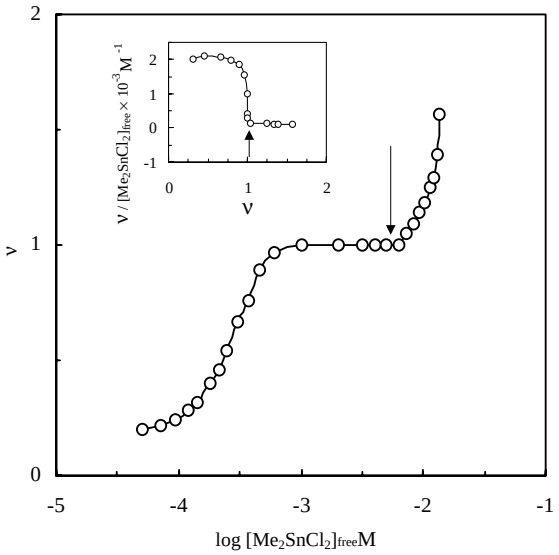

Fig. 2. Binding isotherm (ν vs. log[Me_2SnCl_2]$_{free}$) for DNA–Me_2SnCl_2 complexes where $\nu = [Me_2SnCl_2]_{bound}/[DNA]$ and $[Me_2SnCl_2]_{bound} = [Me_2SnCl_2]_{total} - [Me_2SnCl_2]_{free}$. Inset: scatchard plot for the binding of Me_2SnCl_2–DNA complexes, ν is the binding ratio and $[Me_2SnCl_2]_{free}$ is the free ligand concentration. The arrow shows the change in the interval of the curve, under the effect of different kinds of interactions at low and higher concentrations of ligand upon interaction with DNA.

of DNA at 260 nm (belonging to DNA base chromophores) in the absence and the presence of Me_2SnCl_2 at higher concentrations (>9 mM). The inset of Fig. 1c is shown the difference absorption spectra for the interaction of DNA with Me_2SnCl_2 at higher concentrations.

Fig. 2 is shown the binding isotherm curve as a plot of ν (the average number of Me_2SnCl_2 moles bind to one mole of DNA base pairs) against logarithm of free ligand concentration. The inset of Fig. 2 is shown the Scatchard plot as a cooperative biphasic changes including the existence of two sets of binding sites on DNA–Me_2SnCl_2 complexes.

3.2. IR spectra

The IR spectra features related to DNA and DNA–Me_2SnCl_2 complexes are presented in Fig. 3a and b. The spectra contain peaks 1715, 1650 and 1618 cm^{-1} (attributed to DNA bases) and 1200, 1087, 1053 and 960 cm^{-1} (attributed to phosphate vibration modes) [47]. The peaks relative to phosphate group of DNA nucleotide were altered via interaction of DNA with Me_2SnCl_2 at low concentration (2.2 mM). It is not possible to obtain IR spectrum for the interaction of DNA with Me_2SnCl_2 at higher concentrations of Me_2SnCl_2 because of solid gel formation.

3.3. The effect of Me_2SnCl_2 on the binding of ethidium bromide to DNA

In order to understanding the mechanisms of the Me_2SnCl_2 and DNA interactions, the EB was used as a probe to monitor such interactions. The binding of EB to DNA, as an intercalating dye, is associated with enhancement of its fluorescence intensity [48]. Thus, it is possible to follow EB binding in the presence of Me_2SnCl_2 as a ligand to evaluate the effects of one ligand binding on another. Fig. 4 shows the Scatchard plots belonging to the inhibitory effect of EB binding with DNA in the presence of Me_2SnCl_2 at low and high concentrations. Fig. 4a indicates the noncompetitive inhibition for such interaction at low concentrations of Me_2SnCl_2 (<9 mM). The slope and *X*-intercept indicate the binding constant (*K*) and number of binding sites (*n*), respectively [49]. Thus, the values of K_1 and n_1 are 51675 and 0.45 for the first set of binding at low concentration of ligand. Fig. 4b shows the noncompetitive inhibition of EB binding with DNA in the presence of Me_2SnCl_2 at higher concentrations (>9 mM). The values of K_2, K_3, n_2, and n_3 are equal to 55876, 58569, 0.50, and 0.55 at the corresponding concentrations of Me_2SnCl_2.

3.4. Enthalpy curves

The inset of Fig. 5 shows the biphasic enthalpy curve of DNA upon interaction with Me_2SnCl_2. The first stage is an exothermic process, the minimum at about 9 mM (highest exothermicity) and the maximum at about 16 mM (lowest exothermicity) of Me_2SnCl_2–DNA complexes. For a better explanation of the enthalpy changes during the progression of interaction, the plot of $\Delta H\nu$ ($\Delta H/\nu$) (i.e. enthalpy changes due to the binding of each mole of ligand per each mole of DNA) against ν was drawn. Fig. 5 shows an exothermic process at low concentration of ligand up to 9 mM up to $\nu = 1$, which is followed by an endothermic process (less exothermicity) at higher concentrations of ligand (>9 mM, $\nu > 1$). The exothermic process continued up to $\nu = 1$, which indicates binding of about 1 mol of Me_2SnCl_2 to 2 mol nucleotides of DNA (1 base pair of DNA). Binding of more ligands to DNA at $\nu > 1$ is accompanied with decreasing of exothermicity (up to $\nu = 1.5$). Thereafter, the enthalpy value becomes almost constant demonstrating the saturation of DNA with Me_2SnCl_2 and termination of the interaction.

3.5. Binding sites analysis

Fig. 3 shows the IR spectra of interaction of DNA with Me_2SnCl_2 at low concentrations (2.2 mM), which indicates the binding of ligand to the phosphate groups of DNA [47]. IR spectrum of DNA in the presence of Me_2SnCl_2 confirmed that such interactions at low concentrations arise from binding of DNA phosphate groups to the ligand because of alteration of IR peaks in the phosphate region [47] (see Fig. 3b). These findings are in agreement with the binding of Me_2SnCl_2 to DNA phosphate groups (PO_2^-) at low ligand concentrations (<9 mM) and also with semiempirical calculations on the interaction between $Me_2Sn(IV)_2^+$ and dinuclide triphosphate duplex, mimicking a DNA model system, were performed by PM3 method [50]. The results showed

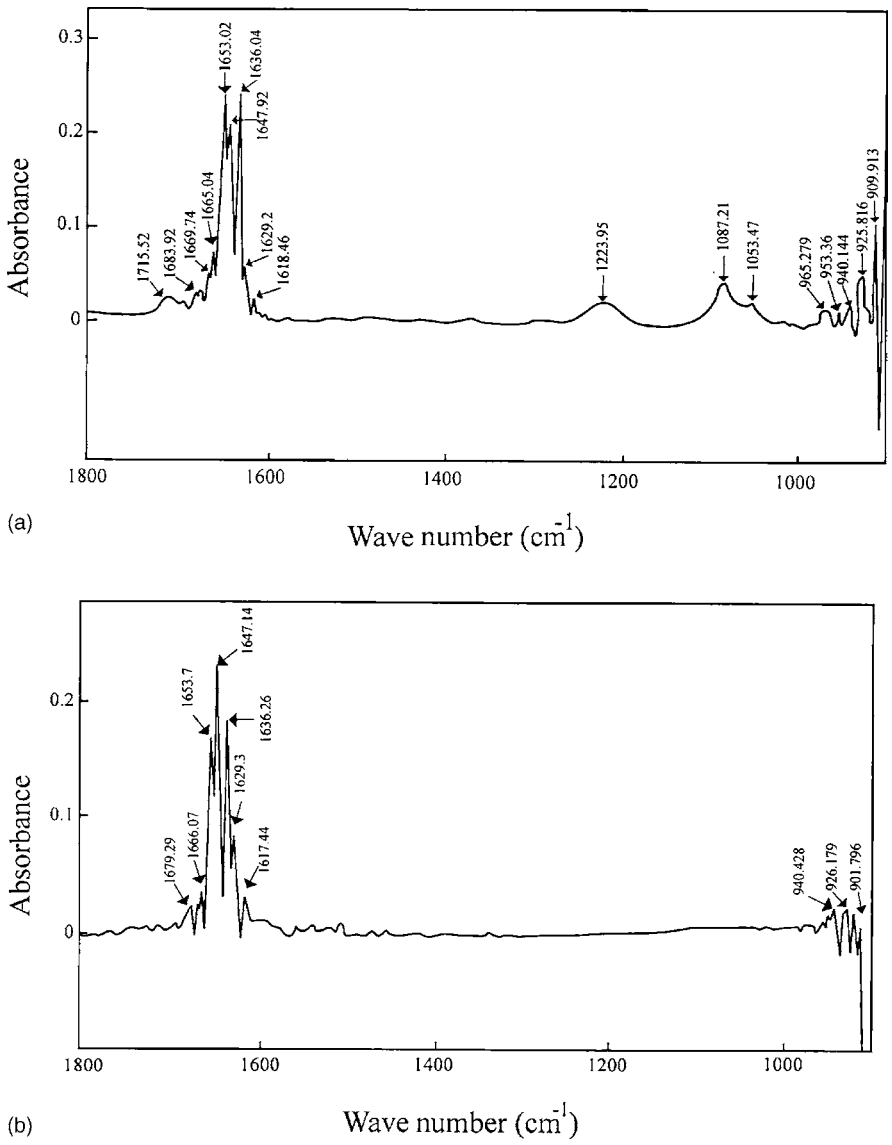

Fig. 3. (a) The IR spectrum of DNA at $pH = 7.6$; (b) the IR spectrum of DNA in the presence of 2.2 mM of Me_2SnCl_2 at pH 7.6.

that the ligand moiety binds to the two adjacent phosphate. An octahedral geometry is proposed for the possible structure of Sn sites in phosphate-bond $R_2Sn(IV)$–DNA. Also Mössbauer and X-ray data have revealed that two water molecules bond to the Sn via oxygen atoms. Binding analysis according to the Hill approach could be also evaluated for such interactions on phosphate groups.

Analysis of binding data according to the Hill model indicated two sets of binding sites (one set for interaction on phosphate groups and one set for nucleotide groups). Hill equation for two sets of binding sites could be written as [51–53]:

$$\nu = \frac{g_1(K_1[L_1])^{n_{H1}}}{1 + (K_1[L_1])^{n_{H1}}} + \frac{g_2(K_2[L_2])^{n_{H2}}}{1 + (K_2[L_2])^{n_{H2}}} \quad (7)$$

where g, K, n_H and $[L]$ denote the maximum number of binding sites, binding constant, Hill coefficient, and Me_2SnCl_2 concentration at corresponding sets, respectively. The inset of Fig. 2 shows the Scatchard plot as a biphasic curve indicating the existence of two sets of binding sites on DNA for Me_2SnCl_2. The first set, which is considered by EB–DNA experiment is a non-intercalative mechanism (i.e. one mole of ligand binds to one mole of DNA base pairs). Therefore, binding of Me_2SnCl_2 on phosphate groups at low concentration (<9 mM) (corresponding up to $\nu = 1$ including two subsites) was associated with an exothermic enthalpy change (see Fig. 5). The interaction was accompanied with some distortion for DNA structure and partial conformational relaxation [54]. Regarding the interaction of DNA with Me_2SnCl_2 at higher concentration (>9 mM), the analysis of binding data according to the Hill model indicated also two sets of binding sites (two sets for nucleotide groups). Hill equation for these two sets of binding sites for such interaction at higher concentration range of ligand could be

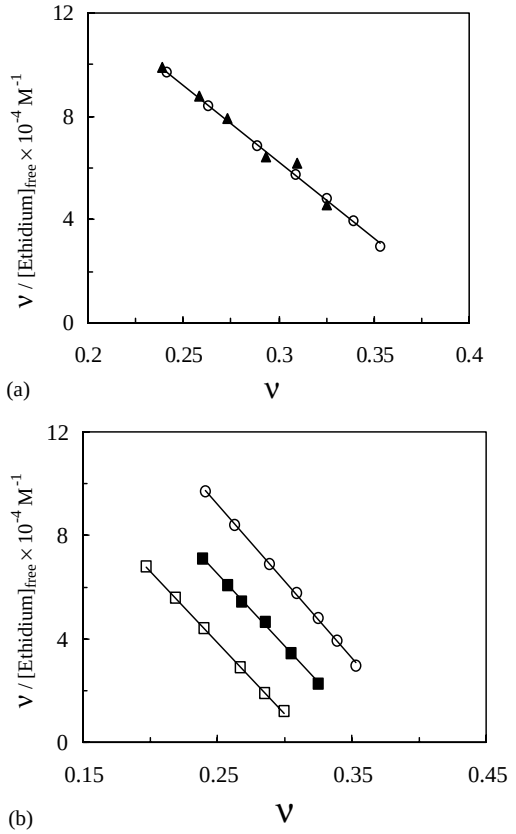

Fig. 4. (a) The Scatchard plots of the binding of ethidium bromide (EB) to DNA at the absence of Me_2SnCl_2 (○), 0.01 mM Me_2SnCl_2 (▲). The Scatchard plot is not altered upon increased concentrations of Me_2SnCl_2 (up to 9 mM) for such interaction (data not shown). The DNA concentration was 0.027 mM bp and EB concentration varied from 2.5 to 21 μM. (b) The Scatchard plots of the binding of ethidium bromide (EB) with DNA in the absence of Me_2SnCl_2 (○); 9.1 mM Me_2SnCl_2 (■) and 9.7 mM Me_2SnCl_2 (□).

written as

$$\nu = \frac{g_3(K_3[L_3])^{n_{H3}}}{1 + (K_3[L_3])^{n_{H3}}} + \frac{g_4(K_4[L_4])^{n_{H4}}}{1 + (K_4[L_4])^{n_{H4}}} \quad (8)$$

The values of g_1–g_4, K_1–K_4, n_{H1}–n_{H4} for corresponding sets were tabulated in Table 1.

In order to elucidate binding sites for DNA–Me_2SnCl_2 complexes we have utilized the Scatchard analysis of the EB–DNA complex in the presence of various concentrations of ligand. The emission of EB–DNA complex as quenched by Me_2SnCl_2 and the Scatchard plots in the absence and the presence of Me_2SnCl_2 showed noncompetitive behavior for such quenching (see Fig. 4).

Previous results are available for Sn(IV)Me_3 [43] and Sn(IV)Me_2 moieties [55]. The hydrolysis of Sn(IV)Me moiety has been studied by ^{1}H and ^{119}Sn NMR spectroscopy and potentiometry [40]. Briefly, from the reported results [43,40] the main, possibly hydrated, species existing in aqueous in pH range 5.0–7.6, may be assumed to be almost the $[Sn(IV)Me_2(OH)]^+$ form and a negligible amount of $SnMe_2(OH)_2$. Also at low concentrations of Me_2SnCl_2

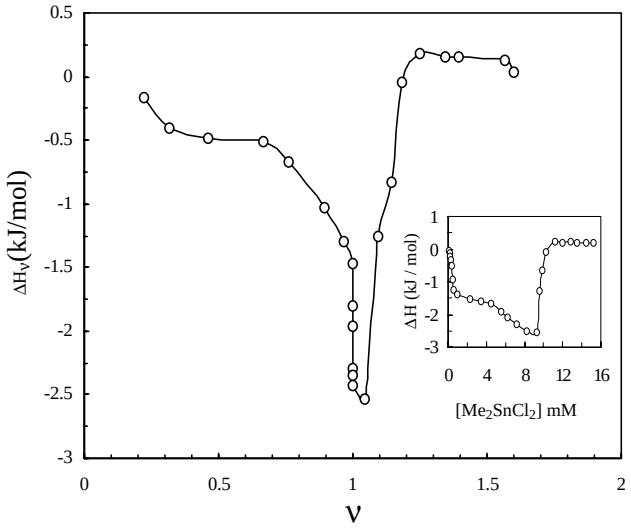

Fig. 5. The calorimetric enthalpy ($\Delta H\nu$) of interaction of Me_2SnCl_2 with DNA at 27 °C. Inset: the enthalpy change versus concentrations of Me_2SnCl_2. The data were obtained from 40 μl in each injection of 3.7 and 55 mM of Me_2SnCl_2 into 1.8 ml solutions for total concentration of Me_2SnCl_2 at <1.22 and >1.22 mM, respectively. The concentration of DNA is 0.0242 mM bp.

the dimeric and trimeric forms can be neglected and only monomeric forms are considered in the solution. Therefore, here $[Sn(IV)Me_2(OH)]^+$ as the main binding specie on interaction with DNA was purposed. By consumption of $[Sn(IV)Me_2(OH)]^+$ the small amounts of $SnMe_2(OH)_2$ can easily convert to the $[Sn(IV)Me_2(OH)]^+$ form at working pH = 7.6. Hence, we assigned Me_2SnCl_2 as a ligand in the text. Binding of organotin(IV) cations to DNA have been reported. For example, coordination of $Me_2Sn(IV)^{2+}$ to 5′-GMP, 5′-ATP, and 5′-[d(CGCGCG)2] and their sugar constituents were investigated in aqueous solution by means of potentiometric titration and H-NMR and P-NMR spectroscopic methods [50]. The results showed that phosphate groups can provide suitable sites for metal ion coordination and at higher concentrations of ligand hydroxyl groups of the sugars or the sugar moieties of the two nucleotides (at alkaline pH) play a role in this process and base moieties of GMP and AMP were not coordinated to $Me_2Sn(IV)^{2+}$ [56].

Here we can say, two kinds of inhibition for such interactions (EB–DNA complex) in the presence of ligand have defined in the literature as follows [49]:

(1) Covalent bonding without chain disruption, which confirms by the coincidence of the experimental points on the unique line either in the absence or in the presence of ligand upon interaction with DNA.
(2) Covalent bonding to the hydroxyl groups of the sugars, the sugar moieties of the two nucleotides [50] which may be illustrated by parallel lines in the absence and presence of ligand (see Fig. 4).

The fact that the slopes of the lines in Fig. 4a and b remain unaltered may be interpreted in the framework of the

Scatchard model to indicate noncompetitive class including the covalent bond between phosphate group of DNA with Me_2SnCl_2 at low concentration of ligand (see Figs. 3b and 4a) and with DNA–Me_2SnCl_2 complexes through bases interaction at higher concentration of Me_2SnCl_2 (see Figs. 4b and 5). This may also block intercalation sites for EB [49]. Such behavior was reported in literature previously by different ligands including some porphyrins [57,58], several platinum and palladium complexes and methylviologen [59]. To confirm such mechanisms, Fig. 5 shows the two kinds of interactions for DNA–Me_2SnCl_2 complexes at low and high ligand concentrations. The first stage at a low concentration of ligand showed the exothermic process and the second stage at a higher concentration of ligand indicated the endothermic contribution. The exothermic process usually shows the electrostatic interaction (DNA outside binding–Me_2SnCl_2 interaction) and endothermic process indicates the transfer of non-polar groups from interior of biomolecules into water [60–62] or unfolding of the biomolecules via hydrophobic contributions [22,60–63]. The decrease in the exothermicity of DNA–Me_2SnCl_2 complexes (>9 mM or $\nu > 1$) belongs to partial unfolding of DNA via interactions with Me_2SnCl_2 at higher concentrations of Me_2SnCl_2 because of low enthalpy values (-2.5289 to $0.2253\,kJ\,mol^{-1}$). Even above 9 mM Me_2SnCl_2, the sign of enthalpy is reversed and then it reaches the stationary state above 16 mM. It must be mentioned that binding of organotin(IV) species at low concentrations is attributed to counter ion binding to DNA phosphodiester [64] with the consequent stabilization of the double helix. While large changes have been reported at high concentrations of the ligand which is interpreted in terms of DNA denaturation due to binding of ligand to DNA sugar moieties as well as to DNA conformational transitions induced by Sn(IV)Me_2 moiety. The results are in agreement with the trends detected in DNA solutions in the presence of a large excess of Ca^{2+} [40] or other main group metal ions. $SnMe_2(OH)_2$ species can be assumed to interact with both hydroxyl and phosphodiester groups [50]. Therefore, our results indicated there are two different behaviors for binding of Me_2SnCl_2 to DNA. An exothermic binding process on phosphate groups took place at low ligand concentrations, while the partial unfolding of DNA occurred via an endothermic (less exothermic) process at higher ligand concentrations.

4. Conclusions

The binding of DNA with Me_2SnCl_2 occurs through two types of interactions in a ligand concentration dependent manner. The outside binding of DNA relative to phosphate group occurs at low ligand concentrations (up to $\nu = 1$), while hydroxyl groups of the sugar, the sugar moieties of the two nucleotides may introduce for interaction at higher ligand concentrations (up to $\nu = 1.5$). Both kinds of interactions have noncompetitive behavior based on Scatchard plots of EB-DNA complexes. Outside binding is accompanied with increasing in exothermic enthalpy, which indicates some compaction on DNA structure during the interaction with Me_2SnCl_2 at low concentrations. However, partial unfolding of DNA takes place because of decreased exothermicity (endothermic process which indicates accessibility of hydrophobic forces to the solvent) at higher ligand concentrations.

Acknowledgements

The authors thank Dr. Christine M. Sorenson and Dr. Nader Sheibani from University of Wisconsin Medical School for their valuable comments. The financial supports from Research Council of the University of Tehran and Islamic Azad University are gratefully acknowledged.

References

[1] V. Ramakarishnan, Annu. Rev. Biophys. Biomol. Struct. 26 (1997) 83–112.
[2] D.P. Mascotti, T.M. Lohman, Biochemistry 36 (1997) 7272–7279.
[3] E. Raspud, M. Olvera, de la Cruz, J.L. Silkarav, F. Livolan, Biophys. J. 74 (1998) 381–393.
[4] H.S. Basu, M. Pellarin, B.G. Feuerstein, A. Shirahata, K. Samejima, D.F. Deen, L.J. Martin, Cancer Res. 53 (1993) 3948–3955.
[5] J.G. Duguid, V.A. Bloomfield, J.M. Benevides, G.J. Thomas Jr., Biophys. J. 69 (1995) 2623–2641.
[6] T. Akao, T. Fukumoto, H. Ihara, A. Ito, FEBS Lett. 391 (1996) 215–221.
[7] S.J. Eastman, C. Siegel, J. Tousignant, A.E. Smith, S.H. Cheng, R.K. Scheule, Biochim. Biophys. Acta 1325 (1997) 41–62.
[8] D.L. Reimer, Y.P. Zhang, S. Kong, J.J. Wheeler, R.W. Graham, M.B. Bally, Biochemistry 34 (1995) 12877–12883.
[9] N. Dan, Biophys. J. 73 (1997) 1842–1846.
[10] P. Edwin, C.M.D. Robert, Biophys. J. 83 (2002) 556–565.
[11] S. Bhattacharya, S.S. Mandel, Indian J. Biochem. Biophys. 34 (1997) 11–17.
[12] S. Bhattacharya, S.S. Mandel, Biochim. Biophys. Acta 1323 (1997) 29–44.
[13] K. Hyakawa, J.P. Saterre, J.C.T. Kwak, Biophys. Chem. 17 (1983) 175–181.
[14] V.D. Osica, T.L. Pyatigorskaya, O.F. Polyvtsev, A.T. Dembo, M.O. Kliya, V.N. Vasilchenko, B.I. Verkin, B.Y. Sukharevsky, Nucleic Acids Res. 4 (1977) 1083–1096.
[15] A.J. Lin, N.L. Slack, A. Ahmad, I. Koltover, C.X. George, C.E. Samuel, C.R. Safinya, J. Drug Target 8 (2000) 13–27.
[16] B.A. Lobo, A. Davis, G. Koe, J.G. Smith, C.R. Middaugh, Arch. Biochem. Biophys. 386 (2001) 95–105.
[17] K. Tsujii, F. Tokiwa, J. Am. Oil Chem. Soc. 54 (1977) 585–586.
[18] M.D. Prager, F.S. Baechtel, W.C. Gordon, S. Maullin, J. Steinberg, A. Sanderson, Liposoms and Immunobiology, Elsevier, New York, 1980, p. 39.
[19] P.G. Arscott, A.Z. Li, V.A. Bloomfield, Biopolymers 30 (1990) 619–630.
[20] V.A. Bloomfield, Biopolymers 31 (1991) 1471–1481.
[21] S.Z. Bathaie, A.A. Moosavi-Movahedi, B. Ranjbar, A.A. Saboury, Colloid Surf.: Biointerf. 28 (2003) 17–25.
[22] S.Z. Bathaie, A.A. Moosavi-Movahedi, A.A. Saboury, Nucleic Acids Res. 27 (1999) 1001–1005.
[23] G.L. Eichhorn, Inorganic Biochemistry, Elsevier, Amsterdam, 1973.

[24] H. Pezzano, F. Podo, Chem. Rev. 80 (1980) 365–401.
[25] A.S. Mildvan, L.A. Loeb, CRC Crit. Rev. Biochem. 6 (1979) 219–244.
[26] S.R. Holbrook, J.L. Sussman, R.W. Warrant, G.M. Church, S.H. Kim, Nucleic Acids Res. 4 (1977) 2811–2820.
[27] T. Lindahl, A. Adams, J.R. Fresco, Proc. Natl. Acad. Sci. U.S.A. 55 (1966) 941–948.
[28] M. Petracopf, K. Hartmut, Chem. Rev. 87 (1987) 1137–1152.
[29] M. Gielen, N.F. Cardarelli, in: N.F. Cavadarelli (Ed.), Tin as a Vital Nutrient: Implications in Cancer Prophylaxis and Other Physiological Processes, CRC Press, Boca Roton, FL, 1986, p. 169.
[30] M.J. Clarke, F. Zhu, D.R. Frasca, Chem. Rev. 99 (1999) 2511–2533.
[31] C. Angela, M.P. Luigi, G. Marcel, K. Martine, W. Rudolph, J. Inorg. Biochem. 85 (2001) 297–300.
[32] M. Gielen, Met. Drugs 5 (1998) 179–188.
[33] A.H. Penninks, W. Seinen, Vet. Q. 6 (1984) 209–219.
[34] Q. Li, P. Yang, H. Wang, M. Guo, J. Inorg. Biochem. 64 (1996) 181–195.
[35] S.J. Blunden, A. Chapman, in: P.J. Craig (Ed.), Organometallic Compound in the Environment, Wiley, New York, 1986, Chapter 3, pp. 111–159.
[36] J.S. Thayer, Organometallic Compounds and Living Organisms, Academic Press, New York, 1984.
[37] S.J. Blunden, P.A. Cusack, R. Hill, The Industrial Uses of Tin Chemicals, The Royal Society of Chemistry, London, 1985.
[38] R. Barbieri, A. Silvestri, J. Inorg. Biochem. 41 (1991) 31–35.
[39] R. Barbieri, A. Silvestri, A. M. Giuliani, V. Piro, J. Chem. Soc., Dalton trans (1992) 585–590.
[40] G. Barone, R. Barbieri, G. La Manna, M.H.J. Koch, Appl. Organometal. Chem. 14 (2000) 189–196.
[41] R. Barbieri, G. Alonzo, R.H. Herber, J. Chem. Soc., Dalton trans. (1987) 789–794.
[42] R. Barbieri, A. Silvestri, V. Piro, J. Chem. Soc., Dalton trans. (1990) 3605–3609.
[43] M.J. Hynes, M. O'Dowd, J. Chem. Soc. Dalton trans. (1987) 563–566.
[44] W.D. Mcfaydyen, N. Sotirellis, W.A. Denny, P.G. Wakelin, Biochim. Biophys. Acta 1048 (1990) 50–58.
[45] K.G. Strothkamp, R.E. Strothkamp, J. Chem. Educ. 71 (1994) 77–79.
[46] A. Schejter, A. Lanir, N. Epstein, Arch. Biochem. Biophys. 174 (1976) 36–44.
[47] H.A. Tajmir-Riahi, A. Rohana, Biopolymers 33 (1993) 1819–1827.
[48] M.J. Waring, J. Mol. Biol. 13 (1965) 269–282.
[49] M. Howe-Grant, K.C. Wu, W.R. Bauer, S.J. Lippard, Biochemistry 15 (1976) 4339–4346.
[50] L. Pellerito, L. Nagy, Coord. Chem. Rev. 224 (2002) 111–150.
[51] A.K. Bordbar, A.A. Moosavi-Movahedi, Bull. Chem. Soc. Jpn. 69 (1996) 2231–2234.
[52] A.A. Saboury, A.K. Bordbar, A.A. Moosavi-Movahedi, Bull. Chem. Soc. Jpn. 69 (1996) 3031–3035.
[53] A.K. Bordbar, A.A. Saboury, M.R. Housaindokht, A.A. Moosavi-Movahedi, J. Colloid Interface Sci. 192 (1997) 415–419.
[54] W. Saenger, Principles of Nucleic Acid Structure, Springer-Verlag, Berlin, 1984.
[55] G. Arena, R. Purrello, E. Rizzarelli, A. Gianguzza, L. Pellerito, J. Chem. Soc., Dalton trans. (1989) 773–777.
[56] A. Jancsó, L. Nagy, E. Moldrheim, E. Sletten, J. Chem. Soc., Dalton trans (1999) 1587–1594.
[57] R.G. Fiel, J. Biomol. Struct. Dyn. 6 (1989) 1259–1275.
[58] R.F. Pasternak, M. Caccam, B. Keogh, T.A. Stephenson, A.P. Williams, E.J. Gibbs, J. Am. Chem. Soc. 113 (1991) 6835–6840.
[59] P. Fromherz, B. Rieger, J. Am. Chem. Soc. 108 (1986) 5361–5362.
[60] D. Freifelder, Physical Chemistry with Application to Biological Science, Jones and Bartlett Publishers Inc., Boston, MA, 1985, p. 173.
[61] G.I. Makhatadze, P.L. Privalov, J. Mol. Biol. 232 (1993) 639–659.
[62] M.N. Jones, Biological Interfaces, Elsevier, Amsterdam, 1975, p. 124.
[63] G.I. Makhatadze, P.L. Privalov, Adv. Protein Chem. 47 (1995) 307–425.
[64] G. Luck, C. Zimmer, Eur. J. Biochem. 29 (1972) 528–536.